A Laplace Distribution-Based Variable Step-Size FxlogLMS Algorithm for Active Impulsive Noise Control

Aoi Haneda* and Yosuke Sugiura† and Tetsuya Shimamura †
* Saitama University, Japan
E-mail: a.haneda.036@ms.saitama-u.ac.jp
† Saitama University, Japan
E-mail: {ysugiura, shima}@mail.saitama-u.ac.jp

***Abstract*—This paper proposes the Laplace Step-size Normalized FxlogLMS+ (LSN-FxlogLMS+) algorithm for Active Noise Control (ANC) in impulsive noise environments. The proposed method features the integration of a novel Variable Step-Size (VSS) mechanism, based on the Laplace distribution, into the robust FxlogLMS+ framework. By combining this Laplace-based VSS with the logarithmic error function, the trade-off between stability and convergence speed is significantly improved.**

Experimental results using both synthetic and real-world impulsive noise confirm that the proposed method achieves superior robustness and faster convergence compared to conventional methods.

I. Introduction

Active Noise Control (ANC) is a widely established technique for attenuating undesired noise in various applications, including personal audio devices, vehicles, and industrial systems. A significant challenge in this field is the mitigation of impulsive noise, which is commonly generated by machinery such as press machines and electric hammers and poses adverse health effects. The foundational algorithm for many ANC systems, the Filtered-x Least Mean Square (FxLMS), is computationally efficient but its performance degrades severely in the presence of such impulsive noise. This type of noise is often modeled theoretically by heavy-tailed Symmetric α-Stable (SαS) distributions.

To address this limitation, two main classes of robust algorithms have been proposed [1]: the Robust Error Functions (REFs) and the Variable Step-Size (VSS) mechanisms. The REF approach, such as FxlogLMS [2], directly applies a non-linear function with sublinear growth to the error signal. This function suppresses the effect of large error values, which contributes to improved robustness in impulsive noise environments.

Building on this, we previously proposed the FxlogLMS+ algorithm [3], which extends FxLMS by introducing a smoothed gradient design. This method demonstrates superior convergence and robustness compared to other REF-based methods like FxLCH [4], NS-FxlogLMS [5], and EFxatanLMS [6].

The second class of algorithms utilizes VSS mechanisms to improve stability by adjusting the step size in response to the input signal's amplitude. A representative example is the FxgsnLMS algorithm [7], which uses a Gaussian function to scale the step-size. However, its convergence speed significantly deteriorates under strongly impulsive noise conditions, as large error values lead to an excessively reduced step-size.

Although REF and VSS strategies are potentially complementary, the integration of a VSS mechanism into the recently proposed FxlogLMS+ algorithm has not yet been explored.

Therefore, we propose the Laplace Step-size Normalized FxlogLMS+ (LSN-FxlogLMS+). This method integrates a new Variable Step-Size (VSS) mechanism, based on the Laplace distribution, into the FxlogLMS+ framework. We selected the Laplace distribution since its heavy tails offer a better trade-off than a Gaussian distribution. This design effectively suppresses extreme outliers while preserving fast convergence.

Through several simulations, we validate the effectiveness of the proposed method. The results demonstrate that the proposed method achieves both fast convergence and high robustness under diverse conditions, ranging from synthetic SαS noise with varying degrees of impulsiveness to real-world industrial noise. It consistently surpasses the performance of the conventional methods, including Th-FxLMS [8], and FxLCH.

II. Conventional Feedforward Active Noise Control

A. Feedforward Active Noise Control System

Figure 1 illustrates the structure of a feedforward ANC system. In this system, the reference microphone and error microphone capture the reference signal $x(n)$ and the error signal $e(n)$, respectively. The secondary loudspeaker generates the control signal $y(n)$ to attenuate the primary noise $d(n)$. The transfer functions $P(z)$ and $S(z)$ represent the primary and secondary paths, respectively. The secondary path model $\hat{S}(z)$ is pre-estimated. The noise control filter $W(z)$ is adaptively updated to minimize the mean power of the error signal.

The filtered reference signal $r(n)$, which passes through the secondary path model, is given by

$$r(n) = \sum_{j=0}^{L-1} \hat{s}(j)x(n-j), \tag{1}$$

979-8-3315-7206-8/25/$31.00 ©2025 IEEE

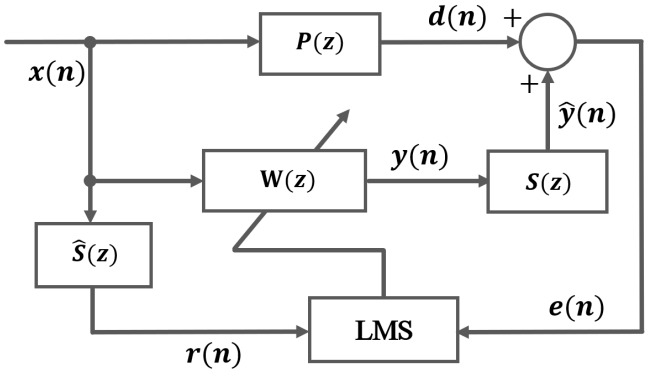

Fig. 1: Block diagram of a feedforward ANC system based on the FxLMS algorithm.

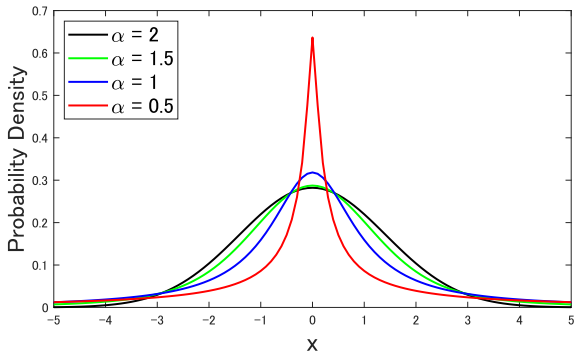

Fig. 2: Probability density functions of the SαS distribution for different values of α: $\alpha = 0.5, 1, 1.5, 2$.

where $\hat{s}(n)$ is the impulse response of the secondary path with a length of L. The k-th coefficient of the noise control filter in the FxLMS algorithm, $w_k(n)$, is updated as

$$w_k(n+1) = w_k(n) - \mu e(n) r(n), \tag{2}$$

where μ is the step-size parameter.

B. α-Stable Noise

The Probability Density Function (PDF) of impulsive noise is often modeled using a SαS distribution, defined as

$$\psi(t) = \mathrm{e}^{-\gamma |t|^{\alpha}}, \tag{3}$$

where $\alpha \in (0, 2)$ controls the kurtosis of the PDF, and $\gamma > 0$ is the scale factor. In this paper, we set $\gamma = 1$.

As α approaches 0, the distribution exhibits strong impulsiveness, whereas for $\alpha \to 2$, it converges to a Gaussian distribution. Some examples of SαS distributions are shown in Fig. 2.

III. Modified FxLMS Algorithm for Active Impulsive Noise Control

Various methods have been proposed to address the limitations of the FxLMS algorithm. This section reviews conventional ANC approaches designed for impulsive noise.

A. Clipping

Clipping-based algorithms operate by constraining the reference and error signals within predefined thresholds. The Threshold-FxLMS (Th-FxLMS) algorithm [8] updates the filter coefficients as

$$w_k(n+1) = w_k(n) - \mu \mathcal{C}(e(n)) \sum_{j=0}^{L-1} \hat{s}(j)\, \mathcal{C}(x(n)). \tag{4}$$

Here, the clipping function $C(\cdot)$ is defined as

$$\mathcal{C}(x) = \max(c_2, \min(c_1, x)), \tag{5}$$

where $c_1 > 0$ and $c_2 < 0$ are the thresholds for the upper and lower bounds.

By applying $\mathcal{C}(\cdot)$, extreme values in $x(n)$ and $e(n)$ are saturated, which helps prevent instability in the filter update. However, its performance is highly sensitive to the choice of the thresholds c_1 and c_2. These thresholds should be tuned to the input signal characteristics, but this tuning process is often challenging and lacks generality. Consequently, VSS and REF-based methods are often preferred in practice.

B. Variable Step-Size

To mitigate the influence of impulsive noise manifesting in the reference signal, VSS methods reduce the step size in response to the large amplitudes in either $x(n)$ or $r(n)$.

The Normalized FxLMS (FxNLMS) algorithm [9], one of the most widely used VSS approaches, adjusts the step size based on the squared norm of the filtered reference signal:

$$\hat{\mu}(n) = \frac{\mu}{\|\mathbf{r}(n)\|_2^2 + \delta}, \tag{6}$$

where δ is a small positive constant to prevent instability due to division by zero.

To further enhance stability, the FxLMS algorithm with Normalized Step-Size (NSS-FxLMS) introduces incorporates the estimated mean power of the error signal $E_e(n)$:

$$\hat{\mu}(n) = \frac{\mu}{\|\mathbf{r}(n)\|_2^2 + E_e(n) + \delta}, \tag{7}$$

where $E_e(n)$ is estimated using an exponential moving average:

$$E_e(n) = \lambda E_e(n-1) + (1-\lambda) e^2(n), \tag{8}$$

where $\lambda \in (0, 1)$ is the forgetting factor.

The General Step-size Normalized FxLMS (FxgsnLMS) algorithm [7] introduces a Gaussian-based normalization to balance stability and convergence speed. The step-size is dynamically adapted according to the input power:

$$\hat{\mu}(n) = \frac{\mu}{\sqrt{2\pi}\sigma} \exp\left(-\frac{x^2(n)}{2\sigma^2}\right), \tag{9}$$

where σ is the standard deviation of the input. As shown in Eq. (9), the step-size decreases exponentially with $x^2(n)$, which suppresses adaptation under high-amplitude noise. However,

this method requires a stability condition on the maximum step-size

$$0 < \mu < \frac{1}{MP_x}, \tag{10}$$

where P_x is the power of the reference signal $x(n)$, and M is the filter order. This constraint limits the upper bound of μ, thereby reducing the maximum achievable convergence speed.

Although VSS methods can mitigate the impact of an impulsive input signal $x(n)$, they fail to counteract the influence of an impulsive error signal $e(n)$ within the gradient term.

C. Robust Error Function

The Robust Error Function (REF) introduces a non-linear mapping to suppress large error amplitudes, enhancing robustness against impulsive noise.

The FxLCH algorithm [4] employs a hyperbolic cosine cost function, which is given by:

$$w_k(n+1) = w_k(n) - \hat{\mu}(n)\tanh(\rho e(n))r(n), \tag{11}$$

where $\hat{\mu}(n)$ follows Eq. (6), and ρ is a positive constant controlling the sensitivity to the error magnitude. Although the $\tanh$ function limits the error term to avoid instability, the unbounded input $r(n)$ can still produce excessively large updates, resulting in performance degradation under impulsive conditions.

To address this issue, FxlogLMS+ [3] extends FxlogLMS by incorporating a normalized logarithmic function into the REF framework. This transformation increasingly attenuates error signals as their magnitude grows, thereby effectively limiting the impact of extreme outliers. The update equation is given by:

$$w_k(n+1) = w_k(n) - \hat{\mu}(n)\psi(e(n))r(n) \tag{12}$$

$$\psi(e(n)) = \mathrm{sgn}(e(n))\frac{\log(G|e(n)|+1)}{G|e(n)|+1}, \tag{13}$$

where G is a gain factor which enhances convergence speed, and $\mathrm{sgn}(\cdot)$ is the sign function. The step-size $\hat{\mu}$ follows Eq.(6).

While REF-based methods such as FxlogLMS+ already incorporate a variable step-size mechanism (e.g., normalized step-size), this is not sufficient to ensure robustness or fast convergence. The VSS must be carefully designed to align with the characteristics of the REF. In particular, the development of a VSS mechanism suitable for FxlogLMS+ remains an important open problem. This is because FxlogLMS+ has demonstrated strong performance as a REF-based algorithm.

IV. Proposed Method

As discussed in the previous section, a suitable VSS mechanism is required for FxlogLMS+.

In this paper, we propose the Laplace Step-size Normalized FxlogLMS+ (LSN-FxlogLMS+). This algorithm introduces a novel VSS employing a function based on the Probability Density Function (PDF) of the Laplace distribution. The Laplace PDF has heavier tails than a Gaussian function. This characteristic better complements the logarithmic REF in FxlogLMS+.

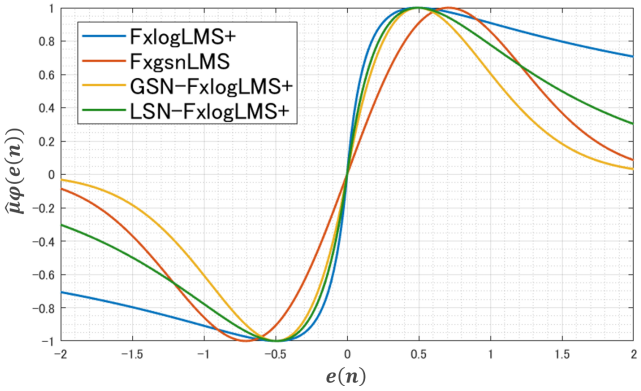

Fig. 3: Comparison of gradient scaling factor for each method.

This compatibility mitigates excessive compression of the step size and contributes to both stable adaptation and fast convergence under impulsive noise.

The update equation of the LSN-FxlogLMS+ is given by

$$w_k(n+1) = w_k(n) - \hat{\mu}(n)\psi(e(n))r(n) \tag{14}$$

$$\hat{\mu}(n) = \frac{\mu}{2b}\exp\left(-\frac{|x(n)|}{b}\right) \tag{15}$$

$$\psi(e(n)) = \mathrm{sgn}(e(n))\frac{\log(G|e(n)|+1)}{G|e(n)|+1}, \tag{16}$$

where $\hat{\mu}(n)$ is Laplace Step-size Normalized (LSN), and, b is the scale parameter.

Unlike Clipping-based methods such as Th-FxLMS, the proposed algorithm employs smoothly adjustable parameters G and b, which offer robustness and tuning flexibility while maintaining stability under various noise conditions.

A. Comparative Analysis of Gradient Scaling Behavior

To investigate the convergence behavior of the proposed algorithm, this section compares its gradient scaling factor, defined as $\hat{\mu}(n)\phi(e(n))$. The benchmarks include FxgsnLMS, FxlogLMS+, and FxlogLMS+ with Gaussian Step-size Normalized (GSN-FxlogLMS+). The GSN-FxlogLMS+ is obtained by replacing the LSN step-size $\hat{\mu}(n)$ in Eq. (14) with the GSN step-size from Eq. (9).

Figure 3 illustrates the resulting gradient scaling curves. For small errors ($|e(n)| \approx 0$), all methods exhibit nearly linear behavior. For large errors ($|e(n)| \gg 0$), however, their suppression characteristics diverge significantly.

The benchmark methods exhibit contrasting characteristics. FxlogLMS+ shows relatively weak suppression, while GSN-FxlogLMS+ exhibits overly strong compression, which can slow down convergence. The proposed LSN-FxlogLMS+ positions itself between these two benchmarks, achieving a more effective trade-off between robustness and convergence speed.

B. Investigation of the Scale Parameter b

The previous subsection established the superiority of the LSN mechanism over the GSN mechanism. This section fur-

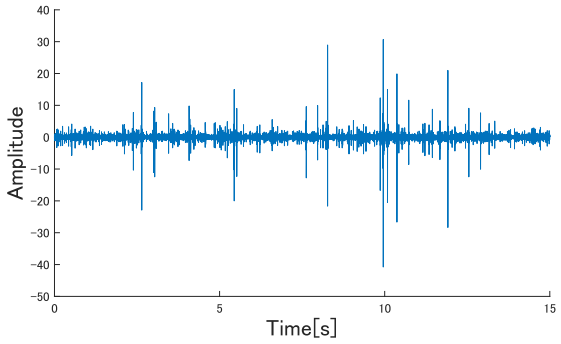

(a) Waveform of reference signal

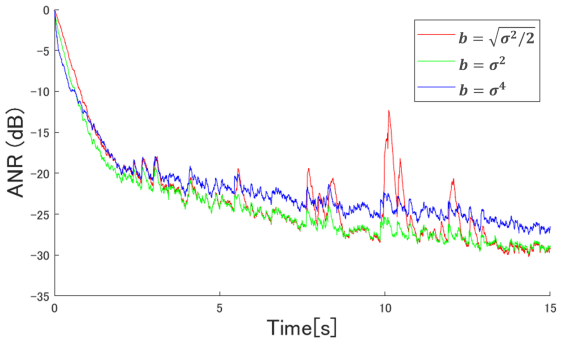

(b) ANR curves

Fig. 4: ANR curves with different settings of b.

ther investigates the optimal value for the core scale parameter, b, to maximize the performance of the LSN framework.

To determine the optimal value for the scale parameter b, we investigate three candidate settings derived from the sample variance of the reference signal $\sigma^2(n)$:

A) $b = \sqrt{\sigma^2(n)/2}$
B) $b = \sigma^2(n)$ (the proposed setting)
C) $b = \sigma^4(n)$

Our hypothesis is that Setting B provides the best trade-off. Setting A may offer insufficient robustness to extreme impulses, while Setting C risks over-suppression that can slow convergence.

Figure 4 shows Averaged Noise Reduction (ANR) over time for each setting. The impulsive noise was generated from an α-stable distribution with α. The ANR is defined as

$$\mathrm{ANR}(n) = 20 \log \frac{A_e(n)}{A_d(n)}, \tag{17}$$

where $A_e(n)$ and $A_d(n)$ are the smoothed amplitudes of primary noise $d(n)$ and error $e(n)$, respectively. They are calculated using a smoothing factor of $\chi = 0.999$ as follows:

$$A_x(n) \quad = \chi A_x(n-1) + (1-\chi)|x(n)|. \tag{18}$$

From Figure 4, the results clearly support our hypothesis. Setting A ($b = \sqrt{\sigma^2(n)/2}$) exhibits a low steady-state ANR, but its ANR spikes sharply when large impulses occur. Conversely, Setting C ($b = \sigma^4(n)$) remains stable against impulsive

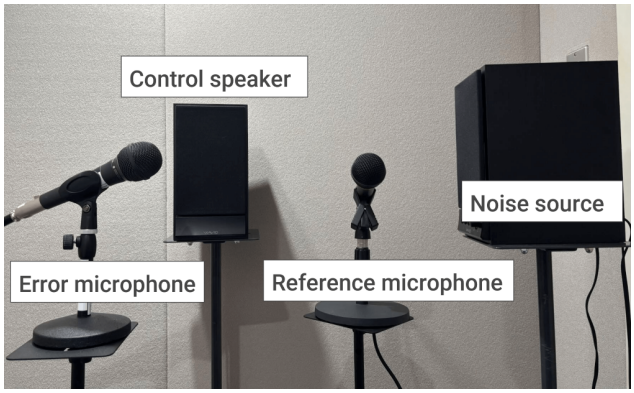

Fig. 5: Experiment Environment.

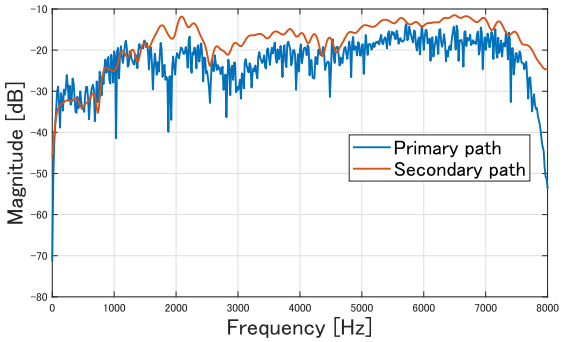

(a) Magnitude reponses of $P(z)$ and $S(z)$

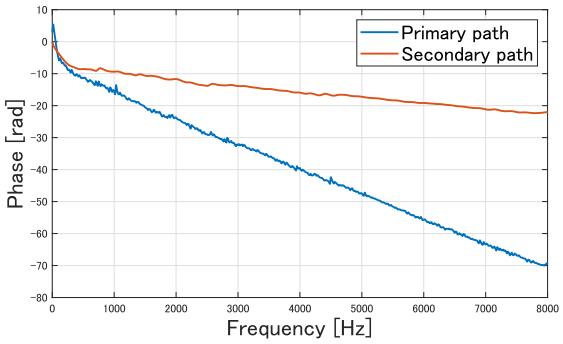

(b) Phase responses of $P(z)$ and $S(z)$

Fig. 6: Frequency responses of the primary path $P(z)$ and secondary path $S(z)$.

noise but exhibits the slowest convergence of the three. Setting B ($b = \sigma^2(n)$), which is the proposed setting, demonstrates both the fastest convergence and the lowest steady-state ANR. This empirically validates Setting B as the optimal choice.

V. EXPERIMENT

To evaluate the effectiveness of the proposed method, we conducted active impulsive noise control simulations. The proposed method was compared against three conventional methods: FxLMS, Th-FxLMS, and LxLCH.

The sampling rate was set to 16 kHz. The acoustic environment, illustrated in Figure 5, included a 20 cm primary

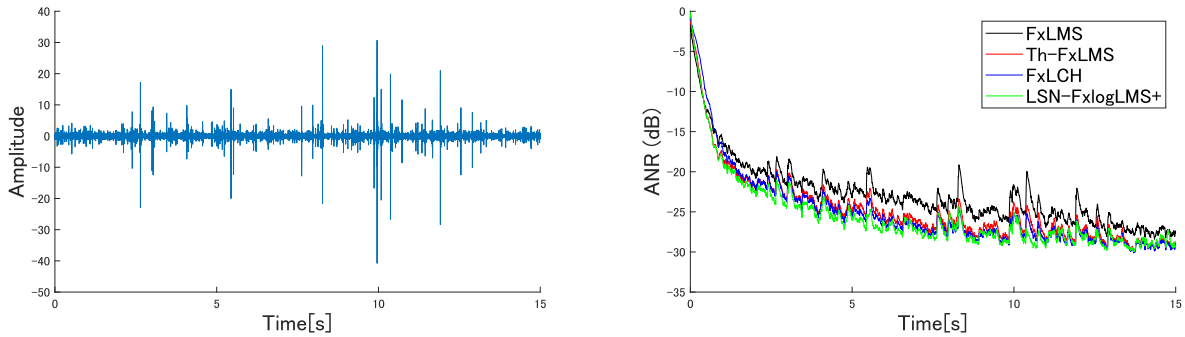

(a) Case 1 : $\alpha = 1.65$ (left: waveform of primary noise, right: ANR curves).

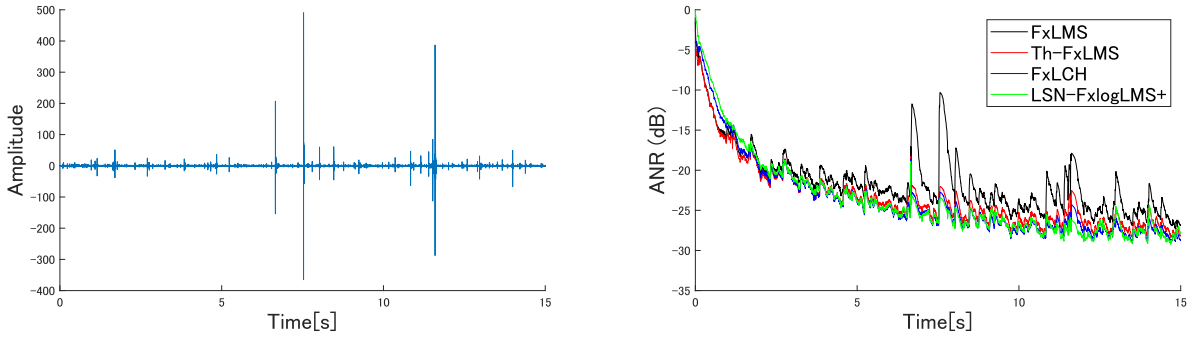

(b) Case 2 : $\alpha = 1.45$ (left: waveform of primary noise, right: ANR curves).

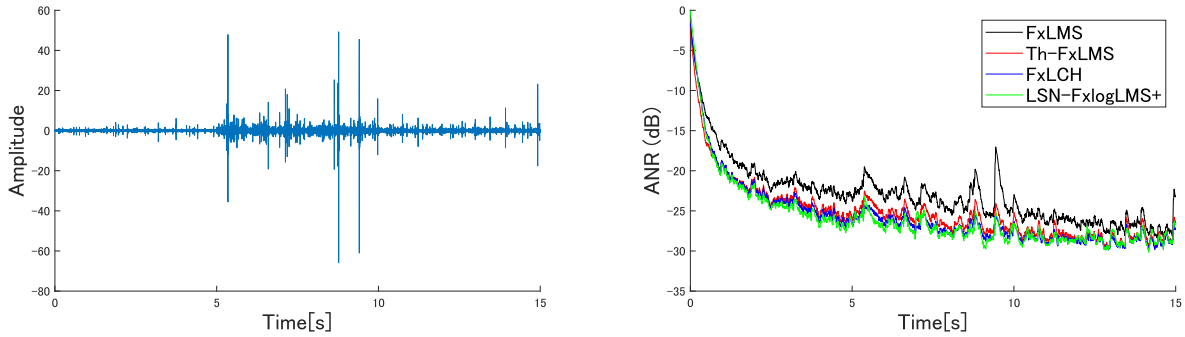

(c) Case 3 : $\alpha = 1.85, 1.45, 1.65$ (left: waveform of primary noise, right: ANR curves).

Fig. 7: Waveform and ANR curves for each method.

path $P(z)$ and a 5 cm secondary path $S(z)$. These paths were modeled using FIR filters with 512 and 128 taps, respectively, and their amplitude and phase characteristics are shown in Figure 6. The control filter length was also 512 taps. For all simulations, the secondary path was assumed to be perfectly estimated (i.e., $\hat{S}(z) = S(z)$).

The performance evaluation was conducted in two parts. Experiment A assesses the algorithm's robustness against theoretical impulsive noise using various α-stable distributions. Experiment B then validates its practical effectiveness using real-world noise recorded from industrial machinery.

A. Performance Evaluation with α-stable Noise

In the first experiment, we evaluated robustness against α-stable noise under three conditions:

- Case 1: $\alpha = 1.65$ (moderately impulsive)
- Case 2: $\alpha = 1.45$ (highly impulsive)
- Case 3: Time-varying α ($1.85 \rightarrow 1.45 \rightarrow 1.65$)

TABLE I: Parameter settings of algorithms.

Algorithm	**Parameters**
FxLMS	$\mu = 0.15$
Th-FxLMS	$\mu = 0.3$, $c_1, c_2 = 0.1$
FxLCH	$\mu = 0.02$, $\rho = 10$
LSN-FxlogLMS+	$\mu = 0.015$, $G = 7.5$

Table I lists the setting parameters for all compared methods.

Figure 7(a)-(c) show the ANR results. The results indicate that while Th-FxLMS and FxLCH achieve a low steady-state ANR, their ANR spikes sharply during impulsive events. In contrast, the proposed LSN-FxlogLMS+ maintains a consistently low ANR across all conditions. This demonstrates its

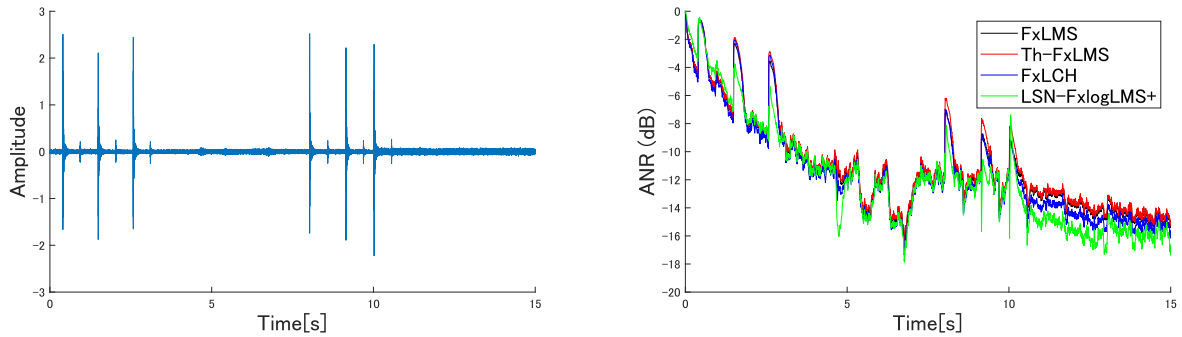

Fig. 8: ANR results of ANC for real-world impulsive noise.

TABLE II: Parameter settings of algorithms.

Algorithm	Parameters
FxLMS	$\mu = 0.01$
Th-FxLMS	$\mu = 0.01$, $c_1, c_2 = 0.1$
FxLCH	$\mu = 0.0007$, $\rho = 10$
LSN-FxlogLMS+	$\mu = 0.0135$, $G = 7.5$

superior robustness and stability against both static and time-varying impulsive noise.

B. Performance Evaluation with Real-World Impulsive Noise

In Experiment B, we validated the method's practical effectiveness using real-world industrial noise. The noise source was a "Valve" sound from MIMII (Malfunctioning Industrial Machine Investigation and Inspection) Dataset [10]. This dataset contains recordings from real factory environments with ambient background noise. The parameters for this experiment are listed in Table II.

Fig. 8 shows the noise waveform and corresponding ANR results. The proposed LSN-FxlogLMS+ again demonstrates the best performance by maintaining the lowest ANR. It is visually confirmed in Figure 8 that the proposed method effectively suppresses not only the stationary background noise but also the sharp, impulsive sounds from the valve.

These result validates the proposed algorithm's effectiveness in a realistic scenario. It successfully handles not only theoretical α-stable noise but also the complex impulsive noise inherent in real-world machinery.

VI. Conclusion

In this paper, we proposed the Laplace Step-size Normalized FxlogLMS+ (LSN-FxlogLMS+) algorithm to improve the performance of Active Noise Control (ANC) in impulsive noise environments. This method integrates a novel Variable Step-Size (VSS) mechanism, based on the Laplace distribution, with the robust FxlogLMS+ framework. Simulation results demonstrated that the proposed algorithm achieves superior robustness and faster convergence under both synthetic α-stable and real-world industrial noise.

References

[1] S. Chen, F. Gu, C. Liang, H. Meng, K. Wu, Z. Zhou, "Review on active noise control technology for α-stable distribution impulsive noise," Circuits, Systems, and Signal Processing, vol. 41, no. 2, pp. 956-993, 2022.

[2] L. Wu, H. He, and X. Qiu, "An active impulsive noise control algorithm with logarithmic transformation," IEEE Trans. Audio Speech Lang. Process., vol. 19, no. 4, pp. 1041–1044, 2011.

[3] A. Haneda, Y. Sugiura, and T. Shimamura, "FxlogLMS+: Modified FxlogLMS Algorithm for Active Impulsive Noise Control." International Conference on Genetic and Evolutionary Computing. Singapore: Springer Nature Singapore, pp. 342-351, 2024.

[4] A. Mirza, A. Zeb, M. Y. Umair, D. Iyas, and S.A. Sheikh, "Less complex solutions for active noise control of impulsive noise," Anal. Integr. Circuits Signal Process., vol. 102, no. 3, pp. 507-521, 2020.

[5] M. Pawelczyk, W. Wierzchowski, L. Wu, X. Qiu. "An Extension to the Filtered-x LMS Algorithm with Logarithmic Transformation," IEEE International Symposium on Signal Processing and Information Technology (ISSPIT), IEEE, 2015.

[6] F. Gu, S. Chen, Z. Zhou and Y. Jiang, "An enhanced normalized step-size algorithm based on adjustable nonlinear transformation function for active control of impulsive noise," Appl. Acoust., vol. 176, 2021.

[7] Y. Zhou, Q. Zhang, and Y. Yin, "Active control of impulsive noise with symmetric α-stable distribution based on an improved step-size normalized adaptive algorithm," Mechanical Systems and Signal Processing, vol. 56, pp. 320-339, 2015

[8] M.T. Akhtar and W. Mitsuhashi, "Improved adaptive algorithm for active noise control of impulsive noise," 9th International Conference on Signal Processing, pp. 2669–2672, 2008.

[9] M.T. Akhtar and W. Mitsuhashi, "A modified normalized FxLMS algorithm for active control of impulsive noise," European Signal Processing Conference (EUSIPCO), pp. 1-5, 2010.

[10] H. Purohit et al., "MIMII Dataset: Sound Dataset for Malfunctioning Industrial Machine Investigation and Inspection," Zenodo, 2019. [Online]. Available: https://doi.org/10.5281/zenodo.3384388.